The IRM Quarterly
Summer 2003, Vol. 13, No. 2

On the tracks of the elusive magnetic oxyhydroxides

Yohan Guyodo loading a sample of As-substituted ferrihydrite in his favorite IRM instrument, the magnetic properties measurement system (MPMS).

Yohan Guyodo
IRM

I came to the IRM as a post-doctoral associate in January 2002, after having spent a little more than four years in Gainesville, Florida, as a Ph.D. student. Needless to say, the transition from the mild winter of North-Central Florida to the glacial January temperatures of Minnesota was a rather traumatizing experience. Surprisingly, however, I managed to survive my first Minnesota winter, perhaps in part because of the warm attitude of the people, or maybe because of the excellent tea that is served occasionally on Fridays at the IRM. At any rate, Minnesota weather can be well avoided if one spends enough time working in the laboratory. During my stay at the IRM, I worked with Subir Banerjee on several projects orbiting around the low-temperature magnetic properties of iron oxyhydroxides. Most of these studies have been conducted through collaboration with Dr. Lee Penn (Chemistry Department) and Dr. Tim LaPara (Civil Engineering Department). Despite the common presence of iron oxyhydroxides in soils and sediments, their detection and quantification in natural samples with traditional characterization methods is often limited due to their low-crystallinity and the inherently poor resolution of their x-ray diffraction spectra (XRD). Highly sensitive methods such as low-temperature rock magnetic techniques may therefore provide a crucial additional tool for the detection and quantification of these minerals in complex mixtures. In the following paragraphs, I will summarize two studies related to my post-doctoral research activities.

One specific project dealt with the growth of goethite nanorods, that is, rod-shaped particles of goethite with an average length of less than a few tens of nanometers. These nanogoethite particles were synthesized by aging a suspension of iron oxyhydroxide nanoparticles for 336 hours at 90ºC (For details, see Guyodo et al., *Geophys. Res. Lett. 30*, 10.1029/2003GL0170212003). The original suspension was obtained in Dr. Penn's laboratory by hydrolysis of a Fe^{3+} solution, following a method developed by Knight and Sylva (1974). This first suspension contained about 89% by number 3.5nm-in-diameter isolated primary particles (referred to as nanodots), and 11% goethite nanorods, with an average width of 3.5nm and an average length of 15.5nm. As mentioned above, this suspension was aged at 90ºC for several days, and samples were taken periodically for analysis with magnetic techniques and with high-resolution transmission electron microscopy (HRTEM). XRD analyses showed that the nanodots were poorly crystalline, and low-temperature magnetometry and susceptometry revealed the superpara-magnetic character of these particles. In the low-temperature susceptibility data, a peak in the in-phase component of the magnetic susceptibility was present around 35K, corresponding to the average blocking temperature of the nanodots (Fig. 1). For increasing aging time, the amplitude of the magnetic susceptibility decreased, which was mostly observed around the susceptibility peak. These results were interpreted in term of a decrease of the number of nanodots with aging time, as confirmed by HRTEM observations. Particle characterization by HRTEM also showed that the decrease of the number of

continued on p. 10...

Suzanne McEnroe
Geological Survey of Norway
Suzanne.McEnroe@ngu.no
Laurie Brown
University of Massachusetts
lbrown@geo.umass.edu

Rock magnetism and magnetic nanostructure of exsolved ilmenite-hematite: Development and testing a realistic atomic hypothesis with implications for magnetic anomaly interpretation on Earth and Mars

Introduction. Proterozoic metamorphic rocks in the Adirondacks (McEnroe and Brown, 2000), pyroxene granulites in SW Sweden (McEnroe et al., 2001a) and hemo-ilmenite-rich rocks in southern Norway (McEnroe et al., 2000, 2001b, 2002) all occur in areas characterized by large negative aeromagnetic anomalies. These rocks are characterized by strong and stable NRM with steep negative inclinations and 75-100% of the NRM remaining after AF demagnetization to 100mT. The fundamental understanding of rocks carrying strong reversed remanence has become important for mineral exploration and interpretation of high-resolution magnetic surveys (Clark, 1997, 1999), and as a primary earth analog for studying the magnetism of Mars. Without a present-day magnetic field, magnetic anomalies observed on Mars must be dominated by remanent components. However, to understand fully remanence-dominated anomalies on Earth, or on other planets, we need to investigate the properties that create and enhance strong magnetic interactions at the atomic scale. In our previous work on negative anomalies in these areas we have found members of the hematite-ilmenite series to be important carriers of remanence, capable of maintaining a stable, strong NRM, despite low concentrations and the presence or absence of magnetite. Rock-magnetic investigations, combined with paleomagnetic and petrographic studies, on samples from strongly magnetized rocks associated with negative anomalies are essential to understand fully the acquisition and characteristics of such remanence.

The question arises as to what mineralogical features are controlling the remanence in these rocks. Members of the hematite-ilmenite solid solution series, and not SD-magnetite, as routinely suggested, are the source of magnetization in these rocks, producing the high coercivity and strong, stable NRM. In these samples, the hematite and ilmenite hosts and lamellae are close to $R\bar{3}c$ titanohematite and $R\bar{3}$ ilmenite below 390°C on the diagram by Harrison (in McEnroe et al., 2002). TEM microstructures show semi-coherent lamellae of ilmenite within a hematite host (or hematite within ilmenite). These are flanked on either side by a precipitate-free zone and abundant fine-scale coherent disk-shaped precipitates of ilmenite-rich material parallel to (001) down to a unit-cell scale of 1-2 nm. The TEM work and modeling suggests that the ultra-fine-scale precipitates of $R\bar{3}$ ilmenite in AF hematite are associated with a 'defect' ferrimagnetic moment due to local imbalance of up and down spins at coherent interfaces (Harrison and Becker, 2000; Robinson et al., 2002 and in revision) which has been called 'lamellar magnetism'. The combined results from these studies strongly suggest that the source of this magnetization is in the exsolution microstructures in these slowly cooled oxides and the strong NRM was acquired at the time of fine exsolution when a magnetic interaction was produced directly at interfaces between paramagnetic ilmenite and antiferromagnetic hematite.

A regional aeromagnetic map of South Rogaland, Norway shows distinct magnetic highs and lows over the 7 km-thick Bjerkreim-Sokndal layered intrusion (BKS). These are related to magnetite-rich layers and hemo-ilmenite rich-layers respectively. A prominent negative anomaly, with an amplitude of -13,000nT in a high-resolution helicopter survey, (up to 27,000nT below background in ground-magnetic profiles), occurs over a hemo-ilmenite norite layer in the BKS (McEnroe et al., in press). TEM work on hemo-ilmenites from the Bjerkreim-Sokndal intrusion shows the same microstructures that have been imaged in the previous studies, possibly enhanced by a strong deformation-induced lattice-preferred orientation of the oxides quasi-parallel to the Proterozoic magnetizing field that would strengthen the 'external force' effect of lamellar magnetism.

What we did at the IRM: We postulate that the process described above is responsible for the magnetism in hemo-ilmenite rocks in Rogaland, both in the hemo-ilmenite ores and in hemo-ilmenite-bearing rocks of the BKS intrusion. We worked on a suite of samples from the BKS intrusion, from pure hemo-ilmenite rocks, and from the surrounding anorthosites. We measured rock-magnetic properties to answer two questions: Are there other magnetic phases than hemo-ilmenite adding to the strong remanence? Do rock-magnetic properties substantiate the ideas presented above for the magnetic interactions between adjacent hematite and ilmenite?

Rock-magnetic measurements were made on 58 samples from 37 sites representing 20 major units in the BKS layered intrusion. Hysteresis properties were measured at room temperature, elevated temperatures and at low temperatures. Samples showed distinct hysteresis loops directly related to mineralogy: 1) hemo-ilmenite, 2) magnetite and 3) magnetite + hemo-ilmenite. After the exclusion of two outliers, samples fell into the range of Mr/Ms from 0.02 to 0.22 and Hcr/Hc from 2 to 10. Elevated temperature hysteresis measurements were made to help us predict what the behavior of these phases would be at depth in the crust in relation to magnetic anomalies. Low-temperature hysteresis measurements were made to look at ordering and to predict the behavior of these minerals at extraterrestrial conditions. Using MPMS, low temperature transitions were studied on selected samples to help determine if small amounts of undetected magnetite were present which could have a controlling effect on the magnetic anomalies. Samples having high Curie and thermal-unblocking temperatures (>580ºC), were studied in further detail at low temperatures to test for magnetic ordering of the nanometer-size hematite lamellae in the hemo-ilmenite samples, using alternating current susceptibilities with 7 frequencies on the MPMS susceptometer from room temperature to 10 K. Lamellae as thin as 1-2 nm traditionally would be considered to behave as SPM grains. However, the highly exsolved samples, both of ilmenite and hematite hosts, showed magnetic ordering at room T, with some dispersion at very lowT related to magnetic ordering in ilmenite and almost none in the hematite hosts. Based on our numerous experiments we conclude that lamellar magnetism, as outlined above, can make an important contribution to the NRM in slowly cooled minerals in the hematite-ilmenite system. This conclusion is of fundamental importance in mineral exploration and planetary magnetism.

References

Clark, D.A., (1997) Magnetic petrophysics and magnetic petrology: Aids to geologic interpretation of magnetic surveys, *Journal of Australian Geology and Geophysics, 17,* 83-103.

Clark, D. A. (1999) Magnetic petrology of igneous intrusions: implications for exploration and magnetic interpreta-

tion. *Exploration Geophysics, 30,* 5-26.
Harrison, R.J. and Becker, U., (2000). Magnetic ordering in solid solutions, *Europe Min.U. Notes in Min, 3,* 369-383.
McEnroe, S. A. and Brown, L.L. (2000*)* A closer look at remanence-dominated aeromagnetic anomalies: Rock-magnetic properties and magnetic mineralogy of the Russell Belt microcline-sillimanite gneiss, Northwest Adirondack Mountains, New York. *J. Geophys Res., 105,* 16,437-16,456.
McEnroe, S. A., Robinson, Peter, and Panish, P. T. (2000) Chemical and petrographic characterization of ilmenite and magnetite in oxide-rich cumulates of the Sokndal region, Rogaland, Norway. *NGU Bull., 426,* 49-56.
McEnroe, S. A., Harrison, R. J., Robinson, P., Golla, U. and Jercinovic, M. J., (2001a) The effect of fine-scale microstructures in titanohematite on the acquisition and stability of NRM in granulite facies metamorphic rocks from Southwest Sweden. *J. Geophys Res., 106,* 30,523-30,546.
McEnroe, S. A., Robinson, Peter and Panish, P. T., (2001b) Aeromagnetic anomalies, magnetic petrology and rock-magnetism of hemo-ilmenite and magnetite rich cumulates from the Sokndal region, South Rogaland, Norway. *Am Min., 86,* 1447-1468.
McEnroe, S. A., Harrison, R., Robinson, Peter and Langenhorst, Falko, (2002), Nanoscale hematite-ilmenite lamellae in massive ilmenite rock: an example of "lamellar magnetism" with implications for planetary magnetic anomalies, *Geophys. J. Int*., 151, 890-912.
McEnroe, S. A. Brown, L.L. and Robinson, Peter, Earth analog for Martian magnetic anomalies: Remanence properties of hemo-ilmenite norites in the Bjerkreim Soknadal Intrusion, Rogaland Norway, J. Applied Geophysics, in press.
Robinson, Peter, Panish, P. T and McEnroe, S. A., (2001) Oxide mineral chemistry of hemo-ilmenite- and magnetite-rich cumulates from the Soknadal region, South Rogaland, Norway. *Am Min., 86,* 1469-1476.
Robinson, P., Harrison, R. J., McEnroe, S. A. and Hargraves, R., 2002, Lamellar magnetism in the hematite-ilmenite series as an explanation for strong remanent magnetization, *Nature, 418,* 517-520.
Robinson, P., Harrison, R. J., McEnroe, S. A. and Hargraves, R., Nature and origin of lamellar magnetism in the hematite-ilmenite series, *Am Min.*, (in revision).

What is the significance of a pervasive normal polarity in Tertiary remagnetizations?

Charly Aubourg
Université Cergy-Pontoise
Charly.Aubourg @geol.u-cergy.fr

Introduction

Just imagine for a second that the pattern of reversals during the Tertiary is unknown. Then take a wide range of publications dealing with Tertiary remagnetization. Surely you would be quite convinced, paper after paper, that there must have been long periods of normal polarity during the Tertiary…

Of course, we *know* that during the Tertiary, the longest normal chron was shorter than 2 My. and that the reversal rate ranged from 2 to 6 reversals per My. So, how can we explain why so many remagnetizations of normal polarity occurred during the Tertiary? Is this just a mere coincidence?

The lower Jurassic carbonates from the southeastern French alps provide an interesting field to investigate the paradox of normal polarity. The debate until now opposes Katz et al. (2000), Kechra et al. (2003), Henry et al. (2001), Cairanne et al. (2002) who argued for different mechanisms to account for the pervasive normal polarity. With G. Cairanne, J.P. Pozzi, F. Brunet, we decided to test the filtering process of a CRM during reversals. We demonstrated experimentally that partial CRMs add perfectly during the hydrothermal production of magnetite under one magnetic reversal (Cairanne et al., 2003a; Cairanne et al., 2003b). Then, the resulting polarity may be the sum of all polarities in this particular process. Is reversal filtering occurred during natural remagnetization? This question remains open, but we strongly favor this sorting effect, as also proposed initially by Henry et al. (2001).

My work, conducted at the IRM, is in the frame of the filtering project. During my cold holidays with warm colleagues from IRM, I aimed to precise the magnetic mineralogy of remagnetized carbonates from SE French Alps. In addition, I carried out fine thermal demagnetization of NRM. Here are some substantial results.

Magnetic mineralogy

I collected data from MPMS, LakeShore, and µVMS instruments in order to appreciate 1) that magnetite is effectively present in remagnetized carbonates, 2) that SP magnetites are present in significant amounts. As seen in Fig. 1A, the Verwey transition (~120K) points to a titanium-poor magnetite. Ferromagnetic grains such as goethite and siderite are also recognized. Frequency dependency of magnetic susceptibility (Fig. 1B) demonstrates the occurrence of appreciable amounts of SP grains. All these characteristics (pure magnetite, SP) are typically detected in remagnetized carbonates.

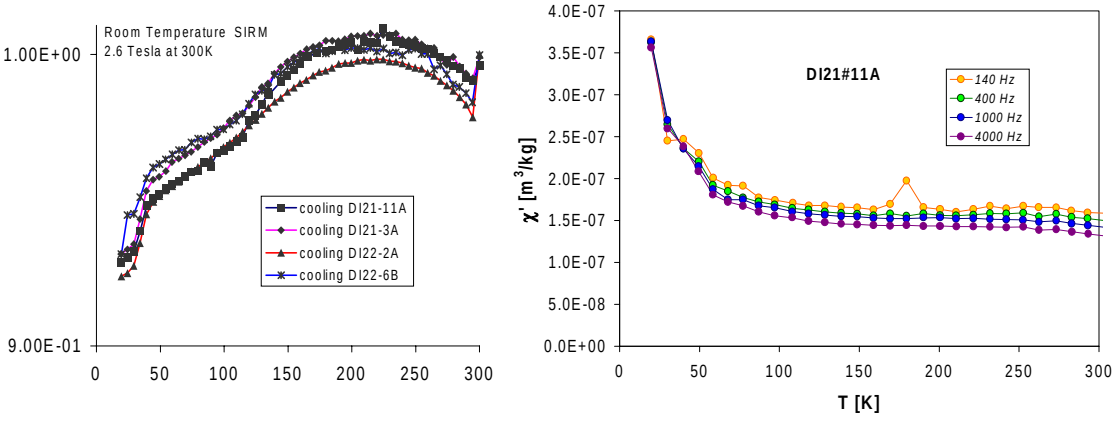

Fig. 1 Thermomagnetic curves of remagnetized carbonates from SE France. A) Cooling of IRM (operated on MPMS). Note the Vervey transition and the sharp drop at ~50K. B) Heating curve of magnetic susceptibility at variable frequency (operated on Lake Shore).

Visiting Fellow Reports
continued on p. 4...

continued from p. 3

Fine demagnetization of NRM.

The goal of this approach was to investigate the possible occurrence of reversals, hidden in a normal polarity remagnetization. I applied a rigorous protocol and measured up to 4 times the same step of temperature. Generally, a continuous decay is observed during demagnetization at 5°C steps (Fig. 2A). Interestingly, we observed a small and significant antipodal component characterized by a zig-zag pattern in the Zijderveld plots and a change of slope of NRM magnitude (see arrow in Fig. 2B).

Conclusion

This set of measurements allows us to better characterize the nature of magnetite in remagnetized carbonates. The finding of a small pure magnetite permits a comparison between remagnetizations observed in SE Alps and experimental CRM with reversals (Cairanne et al., 2003a; Cairanne et al., 2003b).

Acknowledgments

Thanks to the IRM people for their help during my stay.

References

Cairanne, G., Aubourg, C., and Pozzi, J.-P. (2002) Syn-folding remagnetization and the significance of the small circle test: Examples from the Vocontian trough (SE France). Physics and Chemistry of the Earth, Parts A/B/C, 27(25-31), 1151-1159.

Cairanne, G., Brunet, F., Pozzi, J.-P., Aubourg, C., and Besson, P. (2003a) Magnetic monitoring of magnetite nucleation and growth: true or apparent monopolarity of natural CRMs ? EGS-AGU-EUG Joint Assembly, Nice.

Cairanne, G., Brunet, F., Pozzi, J.-P., Besson, P., and Aubourg, C. (2003b) Magnetic monitoring of hydrothermal magnetite nucleation and growth: record of magnetic reversals. American Mineralogist, 88, 1385-1389.

Henry, B., Rouvier, H., Le Goff, M., Leach, D., Macquar, J.C., Thibieroz, J., and Lewchuk, M.T. (2001) Paleomagnetic dating of widespread remagnetization on the southeastern border of the French Massif Central and implications for fluid flow and Mississippi Valley-type mineralization. Geophysical Journal International, 145(2), 368-380.

Katz, B., Elmore, R.D., Cogoini, M., Engel, M.H., and Ferry, S. (2000) Associations between burial diagenesis of smectite, chemical remagnetization, and magnetite authigenesis in the Vocontian trough, SE France. Journal of Geophysical Reasearch, 105(NO. B1), 851-868.

Kechra, F., Vandamme, D., and Rochette, P. (2003) Tertiary remagnetization of normal polarity in Mesozoic marly limestones from SE France. Tectonophysics, 362(1-4), 219-238.

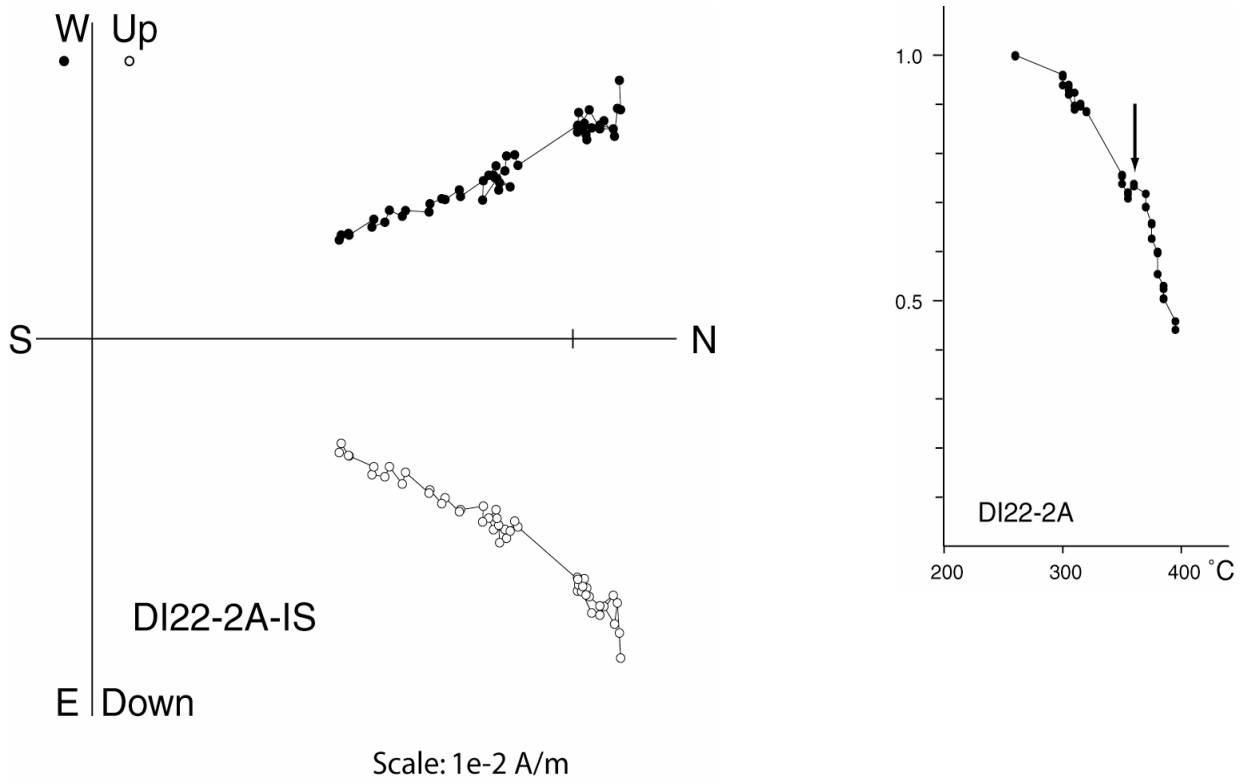

Fig. 2 Fine step demagnetization at 5°C of remagnetized carbonates characterized with a unique normal polarity. A) Zijderveld plot. B) Magnitude of NRM. A small and significant reversal is detected at ~360°C.

The hysteresis properties of multidomain magnetite and titanomagnetite/-maghemite in Mid-Ocean Ridge Basalt

Daming Wang
University of Michigan
wangdm@umich.edu

Titanomagnetite/-maghemites are the main magnetic carriers of mid-ocean ridge basalts (MORB). However, on some occasions low-titanium magnetite has been observed in MORB, notably in massive flows or sills within the oceanic crust. The purpose of my visit was to characterize the rock magnetic properties of a suite of drilled ODP/DSDP basalt samples (97samples from 25 drilling sites) ranging in age between Quaternary to Cretaceous, with the aim to correlate magnetic and electron microscopy data. In addition to hysteresis measurements at room temperature for all the samples, I performed hysteresis measurements at low temperature for selected samples. It is an interesting observation that approximately linear, yet separate, relationships between coercive force (B_c) and the ratio of saturation remanence / saturation magnetization (M_{rs}/M_s) are observed for massive doleritic basalts with low-Ti magnetite and for pillow basalts with multi-domain titanomagnetite/-maghemite (Fig. 1). The existence of low-Ti magnetite in doleritic basalts was confirmed by both Curie temperature measurements and electron microscopy observations. Compilation of hysteresis measurements of fresh pillow basalts and magnetite-bearing doleritic basalts from previous studies confirms that the hysteresis parameters are clearly distinguishable. The parameters for these iron-oxides with different titanium content level reveal contrasting trends that can be explained by the different saturation magnetizations of the mineral types.

Low-temperature hysteresis loops were measured with the MicroMag from 10 K to 400 K. Saturation remanence and coercive force generally increase with decreasing temperature for all the variably-oxidized basalt samples. For relatively fresh (young) and highly-oxidized (old) samples, hysteresis parameters can even share a similar variation trend as a function of temperature (Fig. 2), which contrasts with the values from medium-oxidized samples (also see visitor fellow report, IRM Quarterly, Fall 2000). Saturation magnetization values below 110 K were not shown due to the complexity in paramagnetic correction (Matzka, IRM quarterly, Fall 2000). Because the low-temperature behavior of titanomagnetite/-maghemite can be affected by other factors, such as chemical composition and grain size, the effects of low-temperature alteration are still not clear. On the other hand, low-Ti magnetite-bearing samples exhibit a local minimum in both H_c and M_{rs} at ~120 K due to Verwey transition or passing isotropic point (not shown).

During my hysteresis measurements using MicroMag, offsets in hysteresis loops were occasionally observed. These undesirable effects may not influence an accurate determination of H_c and M_{rs}; however, backfield demagnetization may be severely compromised. The apparent offsets in the readout of magnetic field disappeared once the control software was restarted. Under the watchful eye of Jim Marvin, this abnormal behavior was identified to be caused by a piece of code that periodically resets the analogue-to-digital converter (ADC) value.

I would like to thank Mike, Jim, Peat, and Qingsong for their help and discussions.

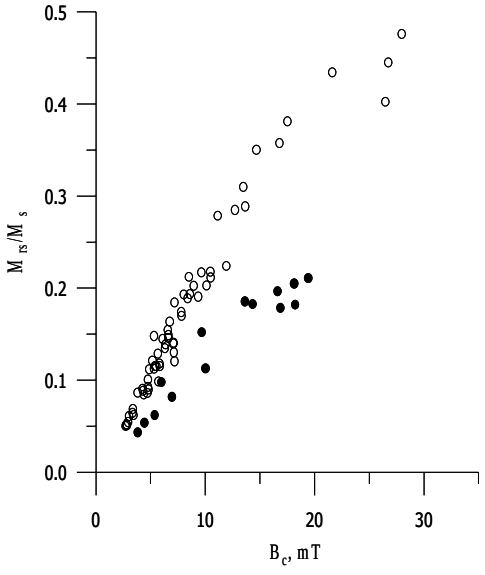

Fig. 1 Reduced saturation magnetization (M_{rs}/M_s) versus coercive force B_c for variably oxidized mid-ocean ridge basalts with TM60 (open symbols) and for basalts with low-Ti or Ti free magnetite (closed symbols).

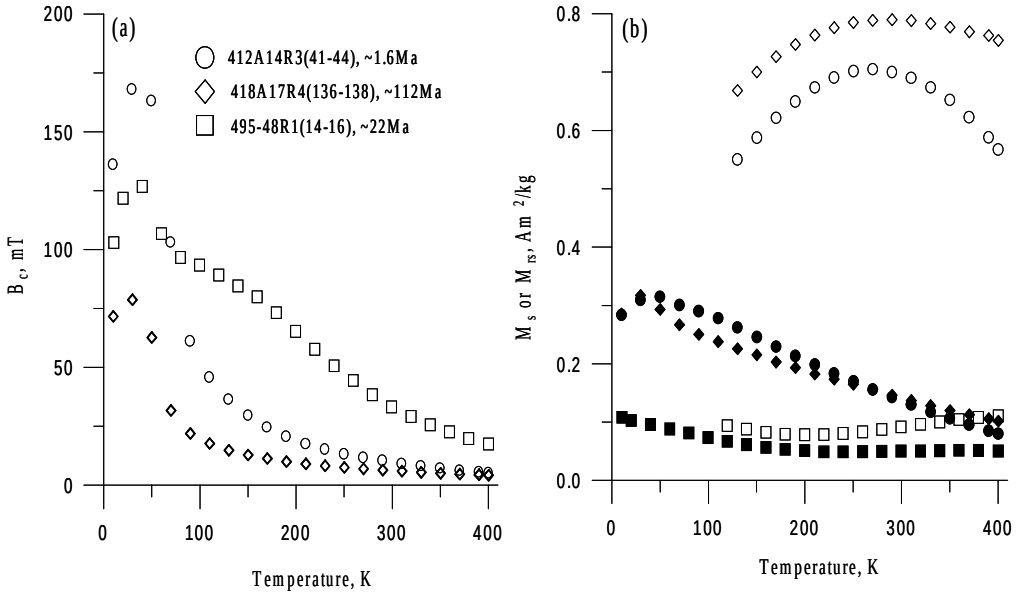

Fig. 2 Low-temperature hysteresis parameters for three representative samples: (a) coercive force as a function of temperature; (b) saturation magnetization (M_s, open symbols) and saturation remanence (M_{rs}, closed symbols) versus temperature.

Fig. 98. Scale ¼.

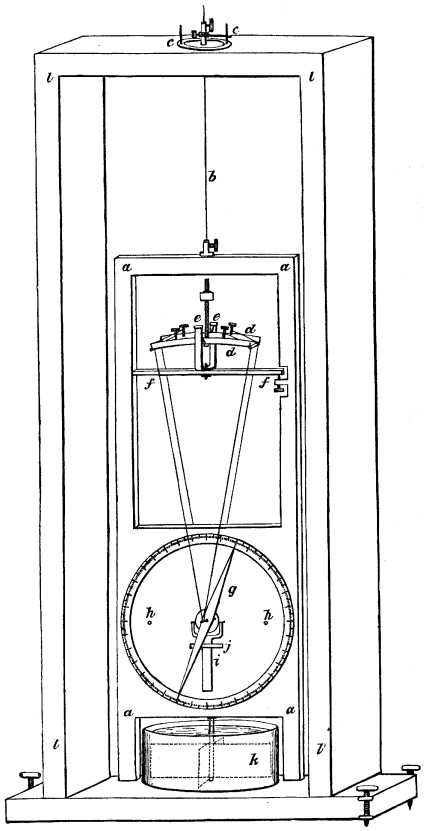

"a needle weighing 63 grains may be hung on silk, and a needle of 16 grains on spider threads. The needle is of softened steel spring in order that it may be thoroughly and uniformly magnetized by two strokes, one on each end, by a magnet protected from actual contact by a covering of silk or leather." Notes on a New Magnetic Dip-Circle, with Experiments, *in* **The Scientific Papers of James Prescott Joule,** The Physical Society of London, 1884.

Current Abstracts

A list of current research articles dealing with various topics in the physics and chemistry of magnetism is a regular feature of the IRM Quarterly. *Articles published in familiar geology and geophysics journals are included; special emphasis is given to current articles from physics, chemistry, and materials-science journals. Most abstracts are culled from* INSPEC *(© Institution of Electrical Engineers),* Geophysical Abstracts in Press *(© American Geophysical Union), and* The Earth and Planetary Express *(© Elsevier Science Publishers, B.V.), after which they are subjected to Procrustean editing and condensation for this newsletter. An extensive reference list of articles (primarily about rock magnetism, the physics and chemistry of magnetism, and some paleomagnetism) is continually updated at the* IRM. *This list, with more than 5200 references, is available free of charge. Your contributions both to the list and to the Abstracts section of the* IRM Quarterly *are always welcome.*

Alteration & Remagnetization

Florindo, F., Roberts, A. P., and Palmer, M. R., 2003, **Magnetite dissolution in siliceous sediments**
Geochemistry Geophysics Geosystems, v. 4, no. 7, 1053, doi:10.1029/2003GC000516.
We have observed low magnetizations in sediments with elevated pore water silica concentrations that arise from diagenesis of biogenic silica and/or silicic volcanic ash. These depletions in magnetization are greater than can be accounted for by dilution with magnetite-poor sediments and suggest that postdepositional destruction of magnetite has occurred. Thermodynamic calculations indicate that magnetite is unstable under conditions of elevated dissolved silica concentrations (and appropriate Eh-pH conditions) and predict that magnetite will break down to produce iron-bearing smectite. A survey of magnetic susceptibility and pore water geochemical data from widely distributed ODP sites supports this.

Lewchuk, M. T., Evans, M., and Elmore, R. D., 2003, **Synfolding remagnetization and deformation: results from Palaeozoic sedimentary rocks in West Virginia**
Geophysical Journal International, v. 152, no. 2, p. 266-79.
Optimal differential unfolding at the site mean level yields one group with a nearly pre-folding, or early synfolding, magnetization (> 70% unfolding) that is both circular and concordant with North America's APW path. The second group has a 'variable synfolding' magnetization that is elliptical at the optimum unfolding level and falls off the path. Differences in either the age of remagnetization or VRM contamination cannot account for this result. The sites falling into the pre-folding group are biased towards the the northwest limb, away from small folds and lower dip angle relative to the sites in the synfolding group. The two groups defined by the fold test results also have a relationship with both total strain and strain partitioning.

Yamazaki, T., Abdeldayem, A. L., and Ikehara, K., 2003, **Rock-magnetic changes with reduction diagenesis in Japan Sea sediments and preservation of geomagnetic secular variation in inclination during the last 30,000 years**
Earth Planets & Space, v. 55, no. 6, p. 327-340.
In this 4.4-m sediment core, reductive dissolution of magnetic minerals occurs between 1.2 and 1.6 m in depth (~5-8 ka). A rapid downcore decrease of ARM begins at the shallowest depth, SIRM follows, and a decrease of κ takes place at the deepest levels. Within this zone, the MDF of NRM and the ratios ARM/κ and SIRM/κ also decrease with depth. From low-temperature magnetometry, it is estimated that magnetites with maghemite skin are reduced to pure magnetites prior to dissolution. Paleomagnetic directions seem to have survived the reductive dissolution: the inclination variations closely resemble other secular variation records available around Japan.

Zegers, T. E., Dekkers, M. J., and Bailly, S., 2003, **Late Carboniferous to Permian remagnetization of Devonian limestones in the Ardennes: Role of temperature, fluids, and deformation**
Journal of Geophysical Research Solid Earth, v. 108, no. B7, 2357, doi:10.1029/2002JB002213.
Paleomagnetic results from 42 sites show three separate NRM components. Hysteresis measurements that are consistent with unremagnetized limestones and the low paleotemperature of the area (< 55°C) indicate that component B is a primary Devonian NRM. Carboniferous component C is carried by a magnetite mix that straddles the SD-MD grain-size range, and postfolding Early Permian component P is carried by pyrrhotite that formed as a result of percolation of MVT fluids through these carbonates. Fine-grained magnetite formation, as a by-product of smectite-to-illite conversion in the presence of host-rock-buffered internal fluids during deformation, is the most likely remagnetization mechanism for component C. Pressure solution deformation processes may have enhanced the smectite-to-illite conversion and hence remagnetization.

Anisotropy

Evans, M. A., Lewchuk, M. T., and Elmore, R. D., 2003, **Strain partitioning of deformation mechanisms in limestones: examining the relationship of strain and anisotropy of magnetic susceptibility (AMS)**
Journal of Structural Geology, v. 25, no. 9, p. 1525-1549.
Strain in two Paleozoic limestone units in the central Appalachian orogen is partitioned into bed-normal shortening due to compaction solution strain (≤35.0% shortening), bed-parallel shortening due to tectonic solution strain (≤13.3% shortening), calcite twinning strain (≤5.8% shortening), and grain-boundary-sliding (≤26.7% shortening). AMS fabrics are composites of: (1) a depositional fabric related to preferentially oriented phyllosilicates; (2) a diagenetic and/or compaction fabric formed during burial that is due to preferentially oriented phyllosilicates in solution structures and in the rock matrix; and (3) a tectonic layer-parallel-shortening fabric, also attributed to preferentially oriented phyllosilicates in solution structures and in the rock matrix, as well as twinning of ferroan calcite.

Henry, B., Jordanova, D., Jordanova, N., Souque, C., and Robion, P., 2003, **Anisotropy of magnetic susceptibility of heated rocks**
Tectonophysics, v. 366, no. 3-4, p. 241-258.
Two methods are proposed to determine the AMS of the ferrimagnetic minerals formed or destroyed during successive heating. The first diagonalizes the tensor from the difference between each tensor term before and after heating. The second employs linear regression for each tensor term made with the values obtained throughout a thermal treatment. By comparing this ferrimagnetic fabric with the initial whole rock fabric, we can distinguish cases where heating simply enhances pre-existing fabric from those where thermal treatment induces a different fabric.

Housen, B. A., and Kanamatsu, T., 2003, **Magnetic fabrics from the Costa Rica margin: sediment deformation during the initial dewatering and underplating process**
Earth and Planetary Science Letters, v. 206, p. 1-2.
ODP Leg 170 penetrated the complete sediment section seaward of the Middle Americas Trench (MAT) at one location, and sections through the margin wedge, decollement, and subducting sediments at two locations near the toe of the wedge. Analyses of these sediments and their structures indicated that the margin wedge is not constructed by offscraping of the present incoming sediments, but is an older (perhaps accreted) structure. Nearly the entire section of sediments entering the MAT is thrust beneath the margin wedge. Within the decollement zone, fabric development is localized to the upper few metres, as indicated by higher AMS P values and by fabric orientations. Below the decollement, the uppermost 180 m of the underthrust hemipelagic sediment section is also deformed, as indicated by comparison of fabrics and their orientations between the seaward reference site and the sites that penetrated the decollement.

Nowaczyk, N. R., 2003, **Detailed study on the anisotropy of magnetic susceptibility of arctic marine sediments**
Geophysical Journal International, v. 152, no. 2, p. 302-17.
Intervals of reversed inclinations documented within five arctic marine sediment cores can be interpreted as geomagnetic excursions because all the investigated sediments are characterized by an undisturbed magnetic fabric. Cores from the Arctic Ocean, in particular, exhibit a strong cyclicity in their anisotropy parameters. Here, sand-rich layers are characterized by a low anisotropy, whereas clay rich layers yielded highest anisotropy degrees of up to 9% indicating an AMS mainly controlled by the matrix properties of the sediment. A simple three-axis determination of the AARM on one of these cores yielded an even higher degree of anisotropy of the ferrimagnetic fraction of up to 18%.

Parés, J. M., and van der Pluijm, B. A., 2002, **Phyllosilicate fabric characterization by Low-Temperature anisotropy of magnetic susceptibility (LT-AMS)**
Geophysical Research Letters, v. 29, no. 24, 2215. doi: 10.1029/2002GL015459.
Paramagnetic susceptibility increases significantly with low temperature, which permits precise determination of the paramagnetic AMS of a rock from measurements at liquid nitrogen temperature. We describe a new procedure that measures directional susceptibility in an oriented rock specimen while immersed in liquid nitrogen. This non-destructive method provides a way of characterizing the principal paramagnetic minerals present in a rock, based on temperature-induced changes of the anisotropy degree. Moreover, the method offers a better-resolved relationship between anisotropy degree and grain alignment, which is used to quantify rock fabrics.

Porreca, M., Mattei, M., Giordano, G., De Rita, D., and Funiciello, R., 2003, **Magnetic fabric and implications for pyroclastic flow and lahar emplacement, Albano maar, Italy**
Journal of Geophysical Research Solid Earth, v. 108, no. B5, 2264, doi:10.1029/2002JB002102.
The most recent activity of the Albano maar extends from ~23 ka into the Holocene and produced the small volume, basic, phreatomagmatic Peperino Albano (PA) ignimbrite, and, more recently, phreatomagmatic surge and lahar deposits. AMS results indicate different transport and/or depositional systems for the veneer and valley pond facies in the PA ignimbrite and for the lahar deposits. AMS also demonstrates that flow directions are mainly controlled by the paleotopography. The paleotopographic control has been interpreted in terms of talweg sedimentation even at proximal locations where deposition occurs from dilute pyroclastic flows.

Tan, X., and Kodama, K. P., 2002, **Magnetic anisotropy and paleomagnetic inclination shallowing in red beds: Evidence from the**

Mississippian Mauch Chunk formation, Pennsylvania
Journal of Geophysical Research, v. 107, no. B11, 2311, doi:10.1029/2001JB001636.
Magnetic anisotropy data indicate that these red beds have suffered from a significant amount of paleomagnetic inclination shallowing. Anisotropy of remanence (IRM and TRM) measurements indicate a bedding parallel, foliated magnetic fabric with foliations ranging from 1.1 to 1.35. Thermal demagnetization at 670° C of the IRM isolates the magnetic fabric of the ChRM-carrying grains and indicates stronger foliations (1.15-1.48). Chemical leaching isolates the AMS of the ChRM-carrying grains, which was used to correct the ChRM inclination. The corrected direction results in a Mauch Chunk paleopole (12° N, 108° E) that is consistent with a European igneous paleopole.

Siemes, H., Klingenberg, B., Rybacki, E., Naumann, M., Schafer, W., Jansen, E., and Rosiere, C. A., 2003, **Texture, microstructure, and strength of hematite ores experimentally deformed in the temperature range 600-1100° C and at strain rates between 10^{-4} and $10^{-6}s^{-1}$**
Journal of Structural Geology, v. 25, no. 9, p. 1371-1391.
Polycrystalline hematite samples cored perpendicular and parallel to the foliation were deformed in triaxial compression experiments. The grain size of the main starting material is up to 175 µm. Grain boundaries are intensely serrated. At T ≤ 800°C the grain boundaries become increasingly lobate and the number of r-twins decreases. Dynamic recrystallization starts above 800°C and a foam structure with grain sizes up to 150 µm develops at T≥900°C. Neutron diffraction measurements show a distinct change of the preferred orientation (texture) in compression parallel to the foliation. The original texture is preferentially preserved but with lower densities at T≥1000°C, presumably caused by increasing diffusional flow processes. Perpendicular to the foliation only minor changes of the texture occurred.

Sizaret, S., Yan, C., Chauvet, A., Marcoux, E., and Touray, J. C., 2003, **Magnetic fabrics and fluid flow directions in hydrothermal systems. A case study in the Chaillac Ba-F-Fe deposits (France)**
Earth and Planetary Science Letters, v. 206, no. 3, p. 555-70.
In these deposits hydrothermal textures and tectonic structures have been described in veins, sinters, and sandstone cemented by hydrothermal goethite. Rock magnetic investigations show that the principal magnetic carrier is goethite for the hydrothermal mineralization and for the laterite level. AMS measurements show distinguishable behaviors in the different mineralogical and geological contexts. Combining the AMS results with vein textures and field data a model is proposed in which AMS results are interpreted in terms of hydrothermal fluid flow. Textural study combined with efficient AMS fabric measurements should be used for systematic investigation to trace flow direction in fissures and in sand porosity.

Biogeomagnetism

Hansel, C. M., Benner, S. G., Neiss, J., Dohnalkova, A., Kukkadapu, R. K., and Fendorf, S., 2003, **Secondary mineralization pathways induced by dissimilatory iron reduction of ferrihydrite under advective flow**
Geochimica et Cosmochimica Acta, v. 67, no. 16, p. 2977-2992.
During dissimilatory iron reduction of 2-line ferrihydrite by *Shewanella putrefaciens* (strain CN32), under advective flow conditions, secondary mineralization occurs via a coupled, biotic-abiotic pathway primarily resulting in the production of magnetite and goethite with minor amounts of green rust. Sorption of bacterially-generated ferrous iron on ferrihydrite is followed by precipitation of goethite (via dissolution/reprecipitation) and/or magnetite (via solid-state conversion), spatially coupled with the ferrihydrite surface. The secondary mineralization pathways following reductive dissolution of ferrihydrite at a given pH are governed principally by flow-regulated Fe(II) concentration, which drives mineral precipitation kinetics and selection of competing mineral pathways.

Environmental Magnetism and Paleoclimate Proxies

Jordanova, D., Veneva, L., and Hoffmann, V., 2003, **Magnetic susceptibility screening of anthropogenic impact on the Danube river sediments in northwestern Bulgaria - Preliminary results**
Studia Geophysica et Geodaetica, v. 47, no. 2, p. 403-418.
Susceptibility variations in sediment cores show the history of depositional and anthropogenic pollution events. Thermomagnetic κ(T) curves indicate magnetite with T_c of 580°C or oxidized magnetite with T_c of 600°C. The samples showing strong magnetic enhancement are characterized by the predominance of magnetite. Optical microscopy on magnetic extracts shows the presence of small spherical particles, typical for the anthropogenic magnetic phases from high-temperature technological processes.

Jordanova, N. V., Jordanova, D. V., Veneva, L., Yorova, K., and Petrovsky, E., 2003, **Magnetic Response of Soils and Vegetation to Heavy Metal Pollutions - A Case Study**
Environ. Sci. & Technol., in press.
Soil and vegetation samples from the study area are characterized by enhanced magnetic properties, due to the presence of magnetite particles of anthropogenic origin accompanying heavy metal emissions. SEM images and microprobe analyses reveal the presence of a significant amount of particles, containing heavy metals (including iron) in vegetation samples taken close to the main pollution source. Correlation analyses show a statistically significant link (correlation coefficients ranging from 0.6 to 0.7) between magnetic susceptibility and the main heavy metals (Cu, Zn, Pb) in soil samples, indicating that the magnetic susceptibility can provide a proxy method for identifying the relative contribution of industrial pollution in soils and vegetation, that is reliable, inexpensive, and less time-consuming than standard chemical analyses.

Kravchinsky, V. A., Krainov, M. A., Evans, M. E., Peck, J. A., King, J. W., Kuzmin, M. I., Sakai, H., Kawai, T., and Williams, D. F., 2003, **Magnetic record of Lake Baikal sediments: chronological and paleoclimatic implication for the last 6.7 Myr**
Palaeogeography Palaeoclimatology Palaeoecology, v. 195, no. 3-4, p. 281-298.
Magnetostratigraphy of a 601 m core provides a robust chronology from the present back to ~6.7 Ma (270 m) and yields a remarkably constant sediment accumulation rate of 3.9 cm/kyr. For earlier times chronology is more problematic. Susceptibility fluctuations reflect climatic changes that can be matched to the marine oxygen isotope pattern for the last 6.7 Myr. Spectral analysis of the resulting susceptibility time series then indicates that, for the most part, the Milankovitch obliquity signal dominates. However, there is also evidence for significant power in a 'non-Milankovitch' band between 28 and 35 kyr.

Phartiyal, B., Appel, E., Blaha, U., Hoffmann, V., and Kotlia, B. S., 2003, **Palaeoclimatic significance of magnetic properties from Late Quaternary lacustrine sediments at Pithoragarh, Kumaun Lesser Himalaya, India**
Quaternary International, v. 108, p. 51-62.
According to radiocarbon chronology, palaeolake Pithoragarh existed from 35 to 10 kyr BP. Fuzzy c-means cluster analysis enables a subdivision of the Riyasi section into five magnetic zones based on clusters related to the relative contribution of the various magnetic constituents, i.e. coarse- (HEM-C) and ultrafine- (HEM-F) grained hematite, both showing relatively soft magnetic behaviour. The model is as follows: during humid periods, magnetic mineralogy is mainly controlled by HEM-F formed in situ, whereas during colder and more arid conditions detrital input of HEM-C and also HEM-F from the catchment area predominates.

Tang, Y. J., Jia, J. Y., and Xie, X. D., 2003, **Records of magnetic properties in Quaternary loess and its paleoclimatic significance: a brief review**
Quaternary International, v. 108, p. 33-50.
The classic loess sections across the Chinese Loess Plateau indicate that wind-blown loess deposition began close to the base of Matuyama (2.6 Ma). However, progress has also been made in extending the record below the loess into the Red Clay and the aeolian record can now be carried back beyond 7 Ma. It is now possible to propose a quantitative model for the reconstruction of paleoclimate according to the paleoprecipitation deduced from proxy indicators, such as susceptibility fluctuation, grain size, stable isotope composition, CaCO3 content, Rb/Sr, and ratio of CBD-extractable Fe_2O_3 to total Fe_2O_3 (Fe_D/Fe_t).

Zhu, R. X., Matasova, G., Kazansky, A., Zykina, V., and Sun, J. M., 2003, **Rock magnetic record of the last glacial-interglacial cycle from the Kurtak loess section, southern Siberia**
Geophysical Journal International, v. 152, no. 2, p. 335-43.
In the loess and buried soils χ_{FD} is very low and uniform, indicating the absence of SP grains and negligible pedogenic enhancement. The magnetic assemblage is dominated by MD-like magnetite grains. Maghemite and haematite are also present in the buried soils and loess horizons. Goethite may have been formed from gleying or water-logging processes under a cooler and more humid climate. The coarse magnetite grains, which contribute significantly to χ, are probably carried by valley winds and derived from local sources. Thus, the higher susceptibility values in the loess horizons could mainly reflect stronger wind intensity during cold and semi-arid conditions. The lower susceptibility values in the buried soil horizons are also due in part to post-depositional modifications (gleying).

Instruments, Calibration and Techniques

Thomas, R. G., Guyodo, Y., and Channell, J. E. T., 2003, **U channel track for susceptibility measurements**
Geochemistry Geophysics Geosystems, v. 4, no. 6, 1050, doi:10.1029/2002GC000454.
A lightweight, transportable, and inexpensive magnetic susceptibility track for u channel samples utilizes a Sapphire Instruments 3.3 cm square coil having a response function of shape similar to that of the 2G-Enterprises u channel magnetometer, and a half-peak width of 3 cm. The instrument has been calibrated using a u channel standard made of manganese dioxide. The software incorporates automated track control and measurement drift correction.

Sagnotti, L., Rochette, P., Jackson, M., Vadeboin, F., Dinares-Turell, J., and Winkler, A., 2003, **Inter-laboratory calibration of low-field magnetic and anhysteretic susceptibility measurements**
Physics of the Earth & Planetary Interiors, v. 138, no. 1, p. 25-38.
We report an inter-laboratory calibration of two key parameters, K_s and K, using two sets of artificial reference samples: a paramagnetic rare earth salt, Gd_2O_3 and a commercial "pozzolanico" cement containing oxidized magnetite with grain size of less than 0.1 µm. Using Gd_2O_3 the 10 Kappabridges tested prove to be cross-calibrated to within 1%, but with a mean K value that is ca. 6% lower than the tabulated value for Gd_2O_3. Inter-laboratory measurements of standard paleomagnetic plastic cubes filled with cement indicate remarkable differences in the intensity of the newly produced ARMs (with a standard deviation of ca. 21%). Differences in the AF decay rate are likely the major source of these variations, but cannot account for all the observed variability.

Magnetic Field Records and Paleointensity Methods

Morales, J., Goguitchaichvili, A., and Urrutia-Fucugauchi, J., 2003, **An experimental evaluation of Shaw's paleointensity method and its modifications using Late Quaternary basalts**
Physics of the Earth & Planetary Interiors, v. 138, no. 1, p. 1-10.
Absolute paleointensity experiments were carried out using Shaw's method and its modifications on 49 samples selected from a large collection because of their low viscosity index, stable NRM and reversible thermomagnetic curves. Moreover, they previously yielded high quality Thellier paleointensity results. Only 13 samples yielded acceptable results using Shaw's original method; 6 of these fail the test proposed by Tsunakawa and Shaw (1994). Rolph and Shaw's (1985) method gives reliable determination only in one case and no single determination was obtained by Kono's (1978) modification. The extremely low success rate of Shaw's paleointensity method may be due to magneto-chemical changes that occurred during heating of samples above their Curie temperatures.

Pan, Y., Shaw, J., Zhu, R., and Hill, M. J., 2002, **Experimental reassessment of the Shaw paleointensity method using laboratory-induced thermal remanent magnetization**
Journal of Geophysical Research, v. 107, no. B7, doi:10.1029/2001JB000620.
Artificial TRM imposed on natural basalt samples was used to check the reliability of Shaw's palaeointensity method. The samples were divided in to three subsets (A, B, and C) and different TRM acquisition parameters were used for each. Rock-magnetic properties on 14 representative subsamples were also measured both before and after the TRM acquisition steps to monitor possible magnetochemical alteration. The Shaw method gave values close to the expected value in all three sets. The modified method with Rolph and Shaw [1985] correction, i.e., using ratios of ARM given before and after the TRM step, proved to be a powerful approach to correct the TRM capacity changes that result from magnetochemical alteration.

Pan, Y. X., Shaw, J., Zhu, R. X., and Hill, M. J., 2003, **Reply to comment by Y. Yamamoto on ''Experimental reassessment of the Shaw paleointensity method using laboratory-induced thermal remanent magnetization''**
Journal of Geophysical Research Solid Earth, v. 108, no. B5, 2279, doi:10.1029/2002JB002355.

Smirnov, A. V., and Tarduno, J. A., 2003, **Magnetic hysteresis monitoring of Cretaceous submarine basaltic glass during Thellier paleointensity experiments: evidence for alteration and attendant low field bias**

abstracts

continued on p. 8...

Earth and Planetary Science Letters, v. 206, no. 3, p. 571-85.
These SBG samples have very low NRM intensities (<50 μA m^2/kg) and Thellier experiments indicate a very weak (<17 μT) paleofield. However, hysteresis properties show systematic variations over the same temperature range where the rapid TRM acquisition is observed, and low-temperature data show that the Verwey transition becomes more distinct with progressive heatings. We attribute these changes to the partial melting and neocrystallization of magnetic grains in SBG during the thermal treatments, resulting in paleointensity values biased to low values. We further propose that this process is pronounced in Mesozoic SBG (relative to Holocene SBG) because devitrification on geologic time scales lowers the temperature at which neocrystallization can commence.

Yamamoto, Y., 2003, **Comment on ''Experimental reassessment of the Shaw paleointensity method using laboratory-induced thermal remanent magnetization'' by Y. Pan, J. Shaw, R. Zhu, and M. J. Hill**
Journal of Geophysical Research Solid Earth, v. 108, no. B5, 2278, doi:10.1029/2002JB002214.

Yu, Y., Dunlop, D. J., and Özdemir, Ö., 2003, **Are ARM and TRM analogs? Thellier analysis of ARM and pseudo-Thellier analysis of TRM**
Earth and Planetary Science Letters, v. 205, no. 3, p. 325-36.
Thellier analysis of ARM and pseudo-Thellier analysis of TRM have been carried out on a large collection of sized synthetic magnetites and natural rocks. In all samples, the intensity of TRM is larger than that of ARM and the ratio R (=TRM/ARM) is strongly grain size dependent. The best-fit slope (b_{fA}) from pseudo-Thellier analysis of TRM shows a linear correlation with R. The ratio b_{fA}/R yielded approximately correct paleointensities, although uncertainties are larger than in typical Thellier-type determinations. For SD and MD magnetites, AF and thermal stabilities of ARM and TRM are fairly similar. However, for 0.24 μm magnetite, ARM is both much less intense and less resistant to thermal demagnetization than TRM, reflecting different domain states for the two remanences and resulting in severely non-linear Arai plots for Thellier analysis of ARM.

Magnetic Microscopy and Spectroscopy

Badurek, G., Buchelt, R. J., Leeb, H., and Szeywerth, R., 2003, **Neutron interferometric reconstruction of magnetic domain structures**
Physica B: Condensed Matter, v. 335, no. 1-4, p. 114-118.
We propose a new method of investigating domain structures in ferromagnetic solids which combines neutron depolarization concepts with perfect crystal neutron interferometry.

Carvalho, E. S. M. L., Ramos, A. Y., Tolentino, H. C. N., Enzweiler, J., Netto, S. M., and Alves, M. D. C. M., 2003, **Incorporation of Ni into natural goethite: An investigation by X-ray absorption spectroscopy**
American Mineralogist, v. 88, no. 5-6, p. 876-882.
Goethite (α-FeOOH) has the unusual capacity to adsorb and fix ions from migrating solutions. X-ray absorption spectroscopy (XAS) was used to obtain structural information on the local environment around Ni in natural Ni-containing goethite (1.8-4.1 mol% Ni) from Vermelho lateritic deposit of Serra dos Carajas (Brazil) and in synthetic analogues. Nickel was found in essentially the same environment in all natural and synthetic samples, with negligible thermal disorder.

Griscom, D. L., Akiyoshi, A., Homae, T., Kondo, K., Yamanaka, C., Ueno, T., Ikeya, M., Affatigato, M., and Schue, A., 2003, **Fossil natural glasses composed of ferric oxyhydroxides: impactites of the 35.5 million year old Chesapeake Bay crater**
Journal of Non Crystalline Solids, v. 323, no. 1-3, p. 7-26.
EXAFS, XRF, XRD, and Mössbauer data demonstrate that the hard red-brown materials found in cobbles of the upland deposits of eastern Virginia contain goethite (α-FeOOH) in particle sizes ~100-150Å with impurity contents < 5%. We propose that their origin may be linked to the impact of an extraterrestrial object 35.5 million years ago into the area that is now the Chesapeake Bay (CB). The hard red-brown materials are proposed to have been quenched from molten sheets of Fe-oxyhydroxides generated by impact-induced shock waves passing through water rich in suspended ferric-oxyhydroxide particles. A model for the physics of this process is presented.

Grygar, T., Hradilova, J., Hradil, D., Bezdicka, P., and Bakardjieva, S., 2003, **Analysis of earthy pigments in grounds of Baroque paintings**
Analytical And Bioanalytical Chemistry, v. 375, no. 8, p. 1154-1160.
Sixteen samples of orange-red and yellow Fe-oxide pigments were studied by elemental and phase analysis and voltammetry. According to the chemical and phase composition the yellow grounds were natural yellow ochres formed by intense chemical weathering in a moderate climate. Some of the orange-red boles originated in the same way, or by calcination of yellow ochres. Part of the orange-red boles differed significantly, especially in their increased content of Ti, indicating their relation to end products of intense weathering, e.g. laterites formed in a tropical climate. In several orange-red boles the intentional addition of rather coarse-grained haematite to natural ochre by the painters was assumed on the basis of Fe oxide content and crystallinity.

Kuzmann, E., Nagy, S., and Vertes, A., 2003, **Critical review of analytical applications of Mössbauer spectroscopy illustrated by mineralogical and geological examples - (IUPAC technical report)**
Pure & Applied Chemistry, v. 75, no. 6, p. 801-858.
We have developed a new terminology for Mössbauer pattern analysis in order to enhance the performance of qualitative analysis by Mössbauer spectroscopy. Mössbauer parameters are considered as a function of a number of externally adjusted experimental parameters at which the spectrum has been recorded. The basis of analytical classification is the microenvironment, which is determined by an assembly of atoms causing the same hyperfine interactions at one particular class of the Mössbauer probe atoms. Our approach can also help to systematize the Mössbauer data for the identification of individual physicochemical species from the corresponding patterns present in the spectrum.

Lorimier, J., Bernard, F., Niepce, J. C., Guigue-Millot, N., Isnard, O., and Berar, J. F., 2003, **Mixed valences in nanometric ferrites investigated by resonant powder diffraction**
Journal of Applied Crystallography, v. 36, p. 301-307.
The dependence of the absorption-edge position on ion valence in resonant scattering can be used to analyse the ionic composition of complex oxides. As the diffraction spectra are more sensitive to f' than to f", the shift in f' associated with the valence can be used to refine the cation distribution. Below the absorption edge the shape of f' is quite insensitive to other site parameters. High-angle data are important to reach significant variation of the diffraction lines. The feasibility of this method for powder materials was tested using a nanometric powder of magnetite, Fe_3O_4 . More complex ferrites were then investigated and the results compared with neutron diffraction experiments.

Moewes, A., Kurmaev, E. Z., Finkelstein, L. D., Galakhov, A. V., Gota, S., Gautier-Soyer, M., Rueff, J. P., and Hague, C. F., 2003, **X-ray emission spectroscopy study of the Verwey transition in Fe_3O_4**
Journal of Physics: Condensed Matter, v. 15, no. 12, p. 2017-22.
The temperature-dependent Verwey transition in a 500Å (111) thin film of Fe_3O_4 (magnetite) has been studied using soft-X-ray emission spectroscopy at room temperature and below the transition temperature T_V. The Fe L2,3 X-ray emission spectra show an increase in the intensity of the L2 emission relative to the L3 emission below T_V. This is independent of the excitation energy and is attributed to a metal-insulator transition across T_V. Comparison of the Fe L3 emission and O K α spectra with LDA band structure calculations supports the suggestion of charge ordering in Fe_3O_4 at low temperature.

Schetinkin, S. A., Wheeler, E., Kvardakov, V. V., Schlenker, M., and Baruchel, J., 2003, **Observation of the phase coexistence in α-Fe_2O_3 at the Morin transition by synchrotron radiation white beam section topography**
Journal of Physics D Applied Physics, v. 36, no. 10A, p. A118-A121.
Phase coexistence during the spin-reorientation Morin transition in haematite (α-Fe_2O_3) was investigated by observing phase boundary movements under the influence of temperature and of a magnetic field, using synchrotron radiation white beam section topography. The sample was a high quality (111) platelet shaped crystal, 1.1 mm thick. The phase boundaries are observed to move while remaining nearly parallel to (111). Nucleation of the weak ferromagnetic phase and pinning of interphase boundaries on defects located in the bulk of the crystal were observed. The observed behaviour patterns are discussed in terms of the elastic and magnetostatic energies involved.

Magnetization & Demagnetization Processes

Borradaile, G. J., 2003, **Viscous magnetization, archaeology and Bayesian statistics of small samples from Israel and England**
Geophysical Research Letters, v. 30, no. 10, 1528, doi:10.1029/2003GL016977.
The T_{UB}-age relationship for the VRM of limestone blocks in dated archeological structures appears to follow a power law, linearized as $\log_{10}(\tau) \propto b \log_{10}(T_{UB})$. From sites constructed with pelagic chalk from eastern England, precise prior information (b=0.761) is compared with less precise information for much more ancient sites in northern Israel (b=0.873). The collective posterior correlation shows a generalized power law exponent b=0.849. That regression explains 84.9% of the collective variance in age (r^2=0.849). Of course, site-specific calibration is required for archaeological age determinations.

Cairanne, G., Brunet, F., Pozzi, J.-P., Besson, P., and Aubourg C., 2003, **Magnetic monitoring of hydrothermal magnetite nucleation-and-growth: record of magnetic reversals**
American Mineralogist, v. 88, p. 1385-1389.
Hematite reduction in the presence of pyrite and CaO led to the formation of anhydrite and magnetite under hydrothermal conditions in a sealed gold container. For the first time, the hydrothermal magnetite production was monitored magnetically at the run conditions. χ is found to follow an Avrami kinetic law. Application of up to two external field reversals in the course of the reaction shows that partial CRMs are recorded by the sample. The intensity of each partial CRM acquired within a given time interval (under a given field intensity) is proportional to the amount of magnetite produced during that time interval. Alternating magnetic field demagnetization failed at separating these partial CRM's, which are believed to superpose in the (*V*, *Hc*) diagram of Néel.

Dunlop, D. J., 2003, **Stepwise and continuous low-temperature demagnetization**
Geophysical Research Letters, v. 30, no. 11, 1582, doi:10.1029/2003GL017268.
For magnetites with sizes from 1 μm to 135 μm, M(T) changed reversibly on cooling in zero field from T_0 = 300 K to 200 K, and in subsidiary warming-cooling cycles $T_1 \rightarrow T_0 \rightarrow T_1$ for any T_1. Changes in M(T) in cooling from 200 K to 130 K were largely irreversible due to decreasing magnetocrystalline anisotropy which promotes wall unpinning and domain nucleation. LTD is almost complete by 130 K in 20-135 μm magnetites but in 1-14 μm magnetites further LTD occurs on cooling to 120 K as magnetocrystalline easy axes change and domains reorganize at T_V. The inverse thermoremanence (ITRM) of 1-14 μm grains is harder to stepwise LTD than saturation remanence (SIRM), while anhysteretic remanence (ARM) is harder than either; for 20-135 μm multidomain grains, ITRM is softer than SIRM.

Madsen, K. N., 2003, **A reversed gyromagnetic effect in chromium dioxide particles**
Journal of Magnetism and Magnetic Materials, v. 260, no. 1, p. 131-40.
The gyromagnetic properties of CrO_2 recording particles have been investigated and compared to those of γ-Fe_2O_3 , which have previously been subject to similar studies. GRM acquired by anisotropic samples in a static experiment was measured for various peak AF as a function of the angle between the AF and the axis of anisotropy. The asymmetry of GRM curves obtained with non-saturating fields may be related to the incoherent reversal mode of the particles. While the GRM of the γ-Fe_2O_3 particles had the sign expected theoretically, that obtained for CrO_2 was of opposite sign. Possible reasons for the reversed gyromagnetic effect are discussed.

Muxworthy, A. R., Dunlop, D. J., and Özdemir, Ö., 2003, **Low-temperature cycling of isothermal and anhysteretic remanence: microcoercivity and magnetic memory**
Earth and Planetary Science Letters, v. 205, no. 3, p. 173-84.
ARM, partial ARMs and partially demagnetised SIRM, induced at room temperature in PSD and MD magnetite, were cooled in zero field to 50 K and then heated back to room temperature. On cooling through T_V, a sharp increase in the remanence was observed. The relative size of the jump increased as the high-coercive-force fraction was increasingly isolated. This behaviour is interpreted as being due to both an increase in the SD/MD threshold size on cooling through T_V and to the reduction of closure domains in the low-temperature phase. In addition, the memory ratio was found to be higher for the high-coercive-force fraction than the low-coercive-force fraction. In our interpretation, the high-coercivity fraction behaviour is associated with reversible domain re-organisation effects, whilst the low-coercive force fraction's behaviour is associated with irreversible domain re-organisation and (de-)nucleation processes.

Ozima, M., Oshima, O., and Funaki, M., 2003, **Magnetic properties of pyroclastic rocks from the later stage of the eruptive activity of Haruna Volcano in relation to the self-reversal of thermo-remanent magnetization**
Earth Planets & Space, v. 55, no. 4, p. 183-188.
Self-reversing TRM behavior is well correlated with the primary chemical composition (TiO_2-content or x) of the hemoilmenite phenocrysts in the samples. Samples with hemoilmenite of ~30 wt% TiO_2 (x~.0.582) showed various types of TRM including typical intense self-reversed TRM (SRTRM), whereas the samples with x~0.620 showed only weak SRTRM. This result harmonizes with the well-known diagram by Uyeda. Moreover, the hemoilmenites with less than ~31 wt% TiO_2 (x~0.60) are capable to acquire various intensities of SRTRM depending on annealing.

Yu, Y., Dunlop, D. J., and Özdemir, Ö., 2002, **Partial anhysteretic remanent magnetization in**

magnetite. 1. Additivity
Journal of Geophysical Research, v. 107, no. B10, 2244, doi:10.1029/2001JB001249.
We have tested the additivity of pARM for eight synthetic magnetites with mean grain sizes from 65 nm to 18 µm and 18 natural samples. For each sample, total ARM intensity was compared with sums of pARMs of three different types: four conjugate pairs of parallel pARMs; four pairs of perpendicular pARMs; and one set of five neighboring parallel pARMs. In each case, the steady field H was applied over nonoverlapping AF intervals that cover the entire range (0-100 mT) used to produce the total ARM. Additivity of partial ARMS was verified to better than 3% for all the samples, whatever the domain state (SD, PSD, and MD) or composition (ranging from pure magnetite to x = 0.6 titanomagnetite). Verification of the law of additivity of pARMs is an encouraging first step toward validating pseudo-Thellier and other methods of paleointensity determination that use ARM in place of, or in addition to, TRM.

Yu, Y., Dunlop, D. J., and Özdemir, Ö., 2002, **Partial anhysteretic remanent magnetization in magnetite. 2. Reciprocity**
Journal of Geophysical Research, v. 107, no. B10, 2245, doi:10.1029/2001JB001269.
A necessary condition for relative paleointensity determination using ARM methods is reciprocity: a pARM, produced by a dc field H applied over a narrow interval (H_2, H_1) of alternating field (AF), must demagnetize over the same interval (H_2, H_1). Experimentally, we find that pARMs of SD and PSD grains demagnetize mainly between H_2 and H_1, whereas >50% of pARMs of large PSD and MD grains are erased below H_1, giving a low-field tail in the coercivity distribution. Pseudo-Arai plots predicted from experimentally determined distributions of blocking and unblocking fields agreed well with measured pseudo-Thellier results, in particular explaining convex-down MD curves.

Mineral & Rock Magnetism

Caizer, C., and Hrianca, I., 2003, **The temperature dependence of saturation magnetization of γ-Fe_2O_3/SiO_2 magnetic nanocomposite**
Annalen der Physik, v. 12, p. 1-2.
For nanoparticles of γ-Fe_2O_3 isolated in an amorphous SiO_2 matrix, M_S increases strongly on cooling from 300 to 77 K; the relative variation (69.7%) is much higher than that of the bulk ferrite (9.5%). The increase is attributed to the narrowing of the paramagnetic layer that exists at the surface of nanoparticles; this layer exists as a result of the modification of the superexchange interaction between iron ions at the nanoparticle surface, due to the distortion of the crystalline network in the presence of the silica matrix. We propose a core-shell model to explain the abnormal increase of M_S for the nanoparticles compared to bulk γ-Fe_2O_3.

Grogan, K. L., Gilkes, R. J., and Lottermoser, B. G., 2003, **Maghemite formation in burnt plant litter at East Trinity, North Queensland, Australia**
Clays & Clay Minerals, v. 51, no. 4, p. 390-396.
Evidence for the formation of maghemite from goethite due to a bushfire on acid sulfate soil at East Trinity, Australia, is presented. Oxidation of pyrite-bearing acid sulfate soils led to precipitation of goethite-impregnated leaf litter. During a major bushfire, goethite with a crystal size calculated from broadening of the 110 reflection of ~9 nm was converted to microcrystalline maghemite (size 12 nm, 220 reflection) and hematite (17 nm, 104 reflection) in a matrix of partly combusted plant litter. Replication of this natural formation of maghemite from goethite was achieved in the laboratory by burning goethite-impregnated leaf litter.

Kapicka, A., Hoffmann, V., and Petrovsky, E., 2003, **Pressure instability of magnetic susceptibility of pyrrhotite bearing rocks from the KTB borehole**
Studia Geophysica Et Geodaetica, v. 47, no. 2, p. 381-391.
Rocks from depths between 5200 and 7000 m in the KTB hole show an increase in susceptibility of between 20 and 120% upon application of pressure. This unstable behaviour was only detected in samples from this depth interval, which contain both ferrimagnetic and antiferromagnetic phases of pyrrhotite. On the basis of thermomagnetic analysis, magnetic field treatment, optical microscopy and domain observations of undeformed and deformed samples, reasons for this instability are discussed and interpreted in relation to redistribution of internal stresses within the ferrimagnetic phase, resulting in changes in domain wall mobility.

Kosterov, A., 2003, **Low-temperature magnetization and AC susceptibility of magnetite: effect of thermomagnetic history**
Geophysical Journal International, v. 154, no. 1, p. 58-71.
SIRM and χ_{AC} have been measured as a function of temperature between 5 and 300 K for one MD and three PSD magnetite samples after cooling in a zero (ZFC) and in a strong magnetic field (FC), and also after three partial field coolings (PFC) when a magnetic field had been turned on in 300-150, 150-80 and 80-5 K ranges, respectively. For the MD sample, SIRM(5 K) after ZFC is about twice as high as after FC, while χ is higher after FC. This behaviour can be fairly well understood in terms of an easy-axis bias produced by cooling through the T_V in a strong magnetic field. PSD grains show a more complex behaviour, which depends strongly on sample stoichiometry, suggesting that low-temperature switching of easy axes is considerably facilitated in strongly non-stoichiometric magnetite.

McClelland, E., Bardot, L., Erwin, P., and Charnley, N., 2003, **Absence of natural viscous remanent magnetization in multidomain high-titanium magnetites: evidence for domain-wall interactions**
Geophysical Journal International, v. 154, no. 1, p. 104-116.
In lava clasts from North Island, New Zealand, VRM parallel to the present Earth's field is present in most clasts, but is absent in clasts with high-Ti titanomagnetite (~TM55) as the only or the dominant magnetic mineral. These TM55 grains are up to 100 µm in size, with no observable exsolution structures, and are therefore MD. We conclude that, in our natural material, MD TM55 does not acquire VRM. In this material, there is evidently no mode of remagnetization available for VRM acquisition other than thermal activation between whole-grain LEM states, and there is insufficient kinetic energy available at 20°C to effect this activation. This is the first demonstration of this effect.

Rochette, P., Sagnotti, L., Bourot-Denise, M., Consolmagno, G., Folco, L., Gattacceca, J., Osete, M. L., and Pesonen, L., 2003, **Magnetic classification of stony meteorites: 1. Ordinary chondrites**
Meteoritics & Planetary Science, v. 38, no. 2, p. 251-268.
A database of magnetic susceptibility measurements on 971 ordinary chondrites demonstrates that χ can be successfully used to characterize and classify ordinary chondrite meteorites. In ordinary chondrites, this rapid and non-destructive measurement essentially determines the amount of metal in the sample, which occurs in a very narrow range for each chondrite class (though terrestrial weathering can result in a variable decrease in susceptibility, especially in finds). This technique is particularly useful not only for a rapid classification of new meteorites, but also as a check against curation errors in large collections. Magnetic remanence, related to magnetic field measurements around asteroids, is also discussed.

Stewart, S. J., Cernicchiaro, G., Scorzelli, R. B., Poupeau, G., Acquafredda, P., and De Francesco, A., 2003, **Magnetic properties and Fe^{57} Mössbauer spectroscopy of Mediterranean prehistoric obsidians for provenance studies**
Journal of Non Crystalline Solids, v. 323, no. 1-3, p. 188-192.
Obsidian samples from six Mediterranean source-islands have variable magnetic and Mössbauer ssignatures. M_s reaches a maximum ~0.3 emu/g for Palmarola obsidians, and H_c ranges from 46 to 372 Oe for respectively samples from Pantelleria and Palmarola islands. Our analyses show that in a M_r/M_s vs. H_c plot, the data points accumulate in areas that depend on obsidian provenance. The Mössbauer spectra are mainly composed of broad asymmetric doublets, which were fitted assuming two Fe^{2+} and one Fe^{3+} sites. In addition, the obsidians of Melos and Palmarola present a magnetic component attributed to magnetite and/or hematite.

Mineral Physics & Chemistry

Lepage, L. D., 2003, **ILMAT: an Excel worksheet for ilmenite-magnetite geothermometry and geobarometry**
Computers & Geosciences, v. 29, no. 5, p. 673-678.

Majzlan, J., Grevel, K. D., and Navrotsky, A., 2003, **Thermodynamics of Fe oxides: Part II. Enthalpies of formation and relative stability of goethite (α-FeOOH), lepidocrocite (γ-FeOOH), and maghemite (γ-Fe_2O_3)**
American Mineralogist, v. 88, no. 5-6, p. 855-859.
The enthalpy of formation from the elements at 298.15 K of lepidocrocite (γ-FeOOH), maghemite (γ-Fe_2O_3), and goethite (α-FeOOH) have been measured as -549.4±1.4, -808.1±2.0, and -560.7 ± 1.2 kJ/mol, respectively. Combined with the entropies for the studied phases, the Gibbs free energies of formation from the elements at 298.15 K are -489.8±1.2, -480.1±1.4, and -727.9±2.0 kJ/mol, for goethite, lepidocrocite, and maghemite, respectively. Only hematite (α-Fe_2O_3) and goethite have a stability field in the Fe_2O_3-H_2O system at low to moderate pressures; maghemite and lepidocrocite are metastable at all pressures and temperatures.

Pownceby, M. I., Constanti-Carey, K. K., and Fisher-White, M. J., 2003, **Subsolidus phase relationships in the system Fe_2O_3-Al_2O_3-TiO_2 between 1000° and 1300° C**
Journal of the American Ceramic Society, v. 86, no. 6, p. 975-980.
Quenched samples were examined using powder XRD and electron probe microanalytical methods. The main features of the phase relations were: (a) the presence of an M_3O_5 solid solution series between end members Fe_2TiO_5 and Al_2TiO_5, (b) a miscibility gap along the Fe_2O_3-Al_2O_3 binary, (c) an α-M_2O_3(ss) ternary solid-solution region based on mutual solubility between Fe_2O_3, Al_2O_3, and TiO_2, and (d) an extensive three-phase region characterized by the assemblage M_3O_5 + α-M_2O_3(ss) + C_{ss}(ss). A comparison of results with previously established phase relations for the Fe_2O_3-Al_2O_3-TiO_2 system shows considerable discrepancy.

Prelot, B., Villieras, F., Pelletier, M., Gerard, G., Gaboriaud, F., Ehrhardt, J. J., Perrone, J., Fedoroff, M., Jeanjean, J., Lefevre, G., Mazerolles, L., Pastol, J. L., Rouchaud, J. C., and Lindecker, C., 2003, **Morphology and surface heterogeneities in synthetic goethites**
Journal Of Colloid And Interface Science, v. 261, no. 2, p. 244-254.
In a study of the acido-basic and sorption properties of iron oxides, a thorough characterization of two types of goethite powders was performed in several laboratories. Chemical analysis by ICPAES; high-resolution SEM, TEM. and AFM observations; XRD with line width analysis; and argon and nitrogen sorption isotherms were used for that purpose. The main crystallographic faces of goethite particles could be identified as {001}, {101}, and {121}, and their abundance correlated with the distribution of low-pressure argon adsorption local isotherms. These results will be very useful for further studies on the relationship between surface reactivity in aqueous solution and orientation of solid surfaces.

Rochette, P., Fillion, G., Ballou, R., Brunet, F., Ouladdiaf, B., and Hood, L., 2003, **High pressure magnetic transition in pyrrhotite and impact demagnetization on Mars**
Geophysical Research Letters, v. 30, no. 13, 1683, doi:10.1029/2003GL017359.
Using neutron diffraction under pressure at room temperature, we observed that pyrrhotite undergoes a ferrimagnetic to paramagnetic transition at about 2.8 GPa. Complete demagnetization of remanence at the same pressure is confirmed in an independent experiment. Such a process provides a quantitative explanation of the magnetic structure of the Martian Southern Hemisphere assuming that pyrrhotite is the major magnetic mineral and that our static experiments can be extrapolated to dynamic pressure conditions. Indeed, the 3 GPa isobaric line during the two large impacts of Argyre and Hellas separates the magnetized and unmagnetized zones. We also infer a reinterpretation of Martian meteorites paleomagnetic signal.

Sanders, J. P., and Gallagher, P. K., 2003, **Kinetics of the oxidation of magnetite using simultaneous TG/DSC**
Journal of Thermal Analysis & Calorimetry, v. 72, no. 3, p. 777-789.
Kinetics of the oxidation of magnetite (Fe_3O_4) to hematite (α-Fe_2O_3) are studied in air using simultaneous TG/DSC. The mechanism is complex and the differences between the kinetic conclusions and Arrhenius parameters based on either TG or DSC are discussed. Solid state reactivity varies from one source of material to another and the results are compared for two different commercial samples of magnetite, both presumably prepared by wet chemical methods. These materials are much more reactive than material studied previously, which had been coarsened and refined at high temperatures. In that earlier study, the metastable spinel γ-Fe_2O_3 was formed as an intermediate in the oxidation to the final stable form, α-Fe_2O_3.

Modeling and Theory

Egli, R., and Lowrie, W., 2002, **Anhysteretic remanent magnetization of fine magnetic particles**
Journal of Geophysical Research, v. 107, no. B10, 2209, doi:10.1029/2001JB000671.
A new, general theory of ARM based on the work of Jaep [1969] includes the influence of parameters like grain size, coercivity, and mineralogy. An analytical expression for ARM intensity in the special case of very fine particles was derived from this theory, and a good agreement with experimental results and data from the literature was found. For strongly interacting samples, ARM is not useful for characterizing the magnetic grains. However, many sediments have a very low concentration of well-distributed magnetic grains, whose properties control ARM acquisition.

Lanci, L., and Kent, D. V., 2003, **Introduction of thermal activation in forward modeling of hysteresis loops for single-domain magnetic particles and implications for the interpretation of the Day diagram**
Journal of Geophysical Research, v. 108, no. B3, 2142, doi:10.1029/2001JB000944.
Synthetic hysteresis loops were generated by numerically solving the classical Stoner-Wohlfarth model and a thermally activated model for a set of randomly oriented magnetic grains. Although computationally intensive this method allows

abstracts

continued on p. 11...

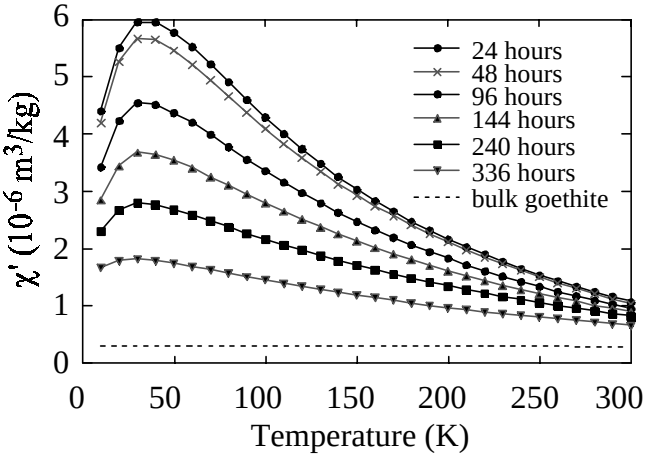

Fig.1: Time evolution of in-phase magnetic susceptibility χ' low-temperature curves (driving field frequency = 1 Hz), for aging times between 24 and 336 hours. Aging of the suspension resulted in a decrease in χ' and a flattening of the curve, converging toward that of bulk goethite (larger crystals of 350nm length).

...oxyhydroxides

continued from p. 1

isolated primary particles was due to oriented aggregation of the nanodots, which resulted in the formation and growth of goethite nanorods. This approach, combining magnetism and microscopy, provided a way to track the nucleation and growth of goethite nanoparticles in this system.

The second project that I would like to mention concerned a comparison between rock magnetic and bacterial community profiles of a modern soil formed over Holocene loess at Prairie Pines, Nebraska (*manuscript in preparation*). Samples for this study were provided by Christoph Geiss from Trinity College. The first series of magnetic measurements consisted of low-field magnetic susceptibility (χ), stepwise alternating field demagnetization of anhysteretic remanent magnetization (ARM), and hysteresis loops in fields up to 1.8T (allowing to determine coercivity, Hc, saturation magnetization, Ms, and saturation remanent magnetization, Mr). Higher values of the ferromagnetic magnetic susceptibility (χ_{ferri}) and lower coercivity values were found at the top of the soil profile, corresponding to the A-horizon, which indicated higher concentration of magnetite and maghemite. As it would be expected for pedogenesis, both ARM/Mr and χ_{ferri}/Ms ratios displayed higher values in that interval, indicating greater amounts of stable single domain/pseudo-single domain and superparamagnetic magnetite particles, respectively (Fig. 2). In addition, low-temperature magnetic measurements with the MPMS indicated both the presence of magnetite and goethite in the samples. In these samples, the presence of goethite was quantified by applying a large magnetic field (here 5T) to the samples, holding the field for temperatures decreasing from 400K (the Néel temperature of goethite) to 300K (room temperature). Then, each sample was demagnetized using an alternating field (AF) with a field peak value of 200 mT, therefore suppressing the part of the signal carried by magnetite, and enhancing the signal carried by magnetically hard but weakly magnetic minerals (e.g., goethite, hematite). Each sample was then cooled down to 10K, warmed up to 400K, and cooled down again. The amount of remanent magnetization carried by the goethite was estimated to be the difference between the magnetization on warming at 300K and the one on cooling back from 400K at the same temperature. In parallel, the soil bacterial community structure profile was analyzed in Dr. LaPara's laboratory by denaturing gradient gel electrophoresis (DGGE) of polymerase chain reaction (PCR) amplified 16S rRNA gene fragments. Our results showed that the bacterial community structure was richly complex and relatively stable down to about 50 cm depth, but changed significantly at greater depth. This shift

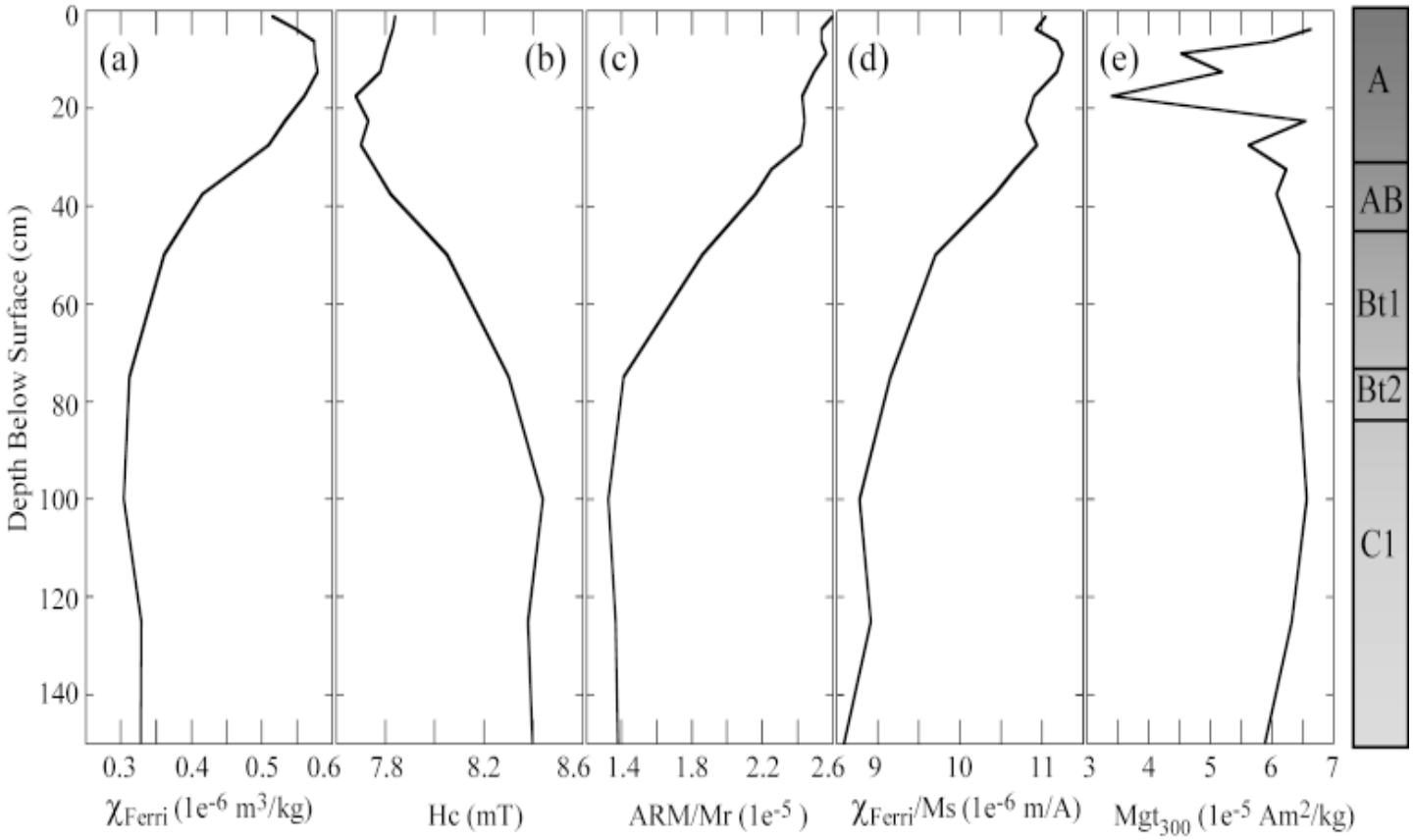

*Fig. 2: Ferrimagnetic mass magnetic susceptibility χ_{Ferri} **(a)**, coercivity Hc **(b)**, ratio of anhysteretic remanent magnetization to saturation remanent magnetization ARM/Mr **(c)**, ratio of ferromagnetic susceptibility to saturation magnetization χ_{Ferri}/Ms **(d)**, and goethite remanent magnetization at 300K Mgt_{300} **(e)** as a function of depth in core. Soil horizons are shown on the right side of the figure.*

Joule, James P.

b. Dec 24, 1818, Manchester
d. Oct 11, 1889, Sale

After studying chemistry with Dalton, Joule followed his father and grandfather into the brewing trade. In his spare time he carried out fundamental and applied research in thermodymanics, electricity and magnetism. Joule's law (1840) relates heat dissipation to wire resistance and the square of current. In 1841 he carried out the first experiments on magnetostriction, concluding that elongation is proportional to the square of magnetization intensity, and that constant volume is maintained by lateral constriction. His famous work on the mechanical equivalent of heat (1840's) was a vital step in establishing the law of conservation of energy. Joule and Thomson (Kelvin) worked in the 1850's on expansion and compression of gases (the "Joule-Thomson effect"). The SI unit of energy is named for Joule.

in bacterial community corresponded to the transition from the A-horizon to the B-horizon, as well as to the measured shift in magnetic parameters. These results were therefore consistent with the idea of a biological contribution to the production of ferrimagnetic minerals in the A-horizon, possibly at the expense of Fe^{3+} minerals such as goethite.

My most recent research activity has been focused on the characterization of synthetic iron oxyhydroxides (e.g., ferrihydrite, goethite) samples produced under a variety of environmental conditions. This work has also involved Mössbauer measurements in collaboration with Peat Solheid (IRM) and Takele Seda (Western Washington University). Our preliminary results indicate that low-temperature magnetic measurements allow distinguishing between samples with different levels of crystallinity, aggregation, and (of course) phase transformation. Evidently, considerable work remains to be done in order to comprehend the magnetism of these minerals, in particular when their average particle size does not exceed a few nanometers. I hope to be able to continue my collaboration with the IRM once installed in my new position at the Laboratoire des Sciences du Climat et de l'Environnement in Gif-sur-Yvette (France). I would like to take this opportunity to thank all the IRM*ers* for providing me with their professional guidance and their friendship during my stay at the University of Minnesota.

forward modeling of hysteresis loops of SD and viscous grains. In the classic Stoner-Wohlfarth model the shape of the modeled loops can be modified by changing the distribution of the anisotropy energy but all the loops have similar hysteresis parameters M_{sr}/M_s and H_{cr}/H_c. Numerical simulation using the thermally activated model changes the shapes of SD loops for sufficiently small particles (≤30 nm, for magnetite), strongly reducing H_c and to a lesser extent the M_{sr}.

Muxworthy, A. R., Dunlop, D. J., and Williams, W., 2003, **High-temperature magnetic stability of small magnetite particles**
Journal of Geophysical Research Solid Earth, v. 108, no. B5, 2281, doi:10.1029/2002JB002195.
The stability of magnetic domain structures of small grains of magnetite were examined between room temperature and the Curie temperature using a high-resolution three-dimensional micromagnetic algorithm. The SD to MD threshold grain size d_0 was found to be nearly independent of temperature up to ~450°C. Above this temperature, d_0 was observed to rise sharply. Transdomain thermoremanence analysis indicated that there are a limited number of grain sizes and shapes which will nucleate domain wall-type structures during cooling. Such nucleation events would cause the total measured remanence to decrease with cooling in conflict with Néel's analytical theory for remanence cooling behavior but in agreement with experimental observations.

Seo, H., Ogata, M., and Fukuyama, H., 2003, **Theory of the Verwey transition in Fe_3O_4**
Physica B: Condensed Matter, v. 329, Part 2, p. 932-933.
The metal-insulator transition in magnetite Fe_3O_4, the so-called Verwey transition, is re-investigated theoretically, motivated by recent experiments. We propose a scenario other than charge order, which has been considered to be its origin so far. We find that the orbital order in the t_{2g} orbitals can make the system effectively one dimensional, so that the bond dimerization is induced due to the Peierls instability. Based on considerations of the elastic energy in the presence of such bond dimer, we argue that an anti-phase configuration of these bond dimer is realized in the actual compound.

NRM Carriers and Origins

Larrasoana, J. C., Pares, J. M., and Pueyo, E. L., 2003, **Stable Eocene magnetization carried by magnetite and iron sulphides in marine marls (Pamplona-Arguis Formation, southern Pyrenees, Northern Spain)**
Studia Geophysica et Geodaetica, v. 47, no. 2, p. 237-254.
Unblocking temperatures suggest that the ChRM is carried by magnetite and iron sulphides. The ChRM has both normal and reversed polarities regardless of whether it resides in magnetite or iron sulphides, and represents a primary NRM acquired before folding. Rock magnetic results confirm the presence of magnetite and smaller amounts of magnetic iron sulphides, most likely pyrrhotite, in all the studied samples. Framboidal pyrite is ubiquitous in the marls and suggests that iron sulphides formed during early diagenesis under sulphate-reducing conditions. ChRM directions carried by magnetic iron sulphides are consistent with those recorded by magnetite. These observations suggest that magnetic iron sulphides carry a CRM that coexists with a remanence residing in detrital magnetite.

Saito, T., Ishikawa, N., and Kamata, H., 2003, **Identification of magnetic minerals carrying NRM in pyroclastic-flow deposits**
Journal of Volcanology & Geothermal Research, v. 126, no. 1-2, p. 127-142.
Type A samples contain titanomagnetite (T_c = 480-485°C), whose grain size is mainly MD. Type B contains Ti-poor titanomagnetite (T_c = 500-580°C), hematite and titanohematite ($Fe_{2-y}Ti_yO_3$) with y~ 0.5 (T_c = 215-220°C). The different magnetic mineral assemblages reflect differences in oxidation state: samples of Type B are strongly oxidized, whereas those of Type A are not. VRM acquisition and demagnetization results indicate that low-coercivity TM in Type A samples acquires VRM easily, whereas titanohematite in Type B hardly acquires VRM. Therefore, the low-temperature NRM component of Type B is not a VRM but a TRM, whose T_{UB} yields an estimate of emplacement temperature between 220 and 400°C.

Synthesis and Properties of Magnetic Materials

Guyodo, Y., Mostrom, A., Penn, R. L., and Banerjee, S. K., 2003, **From Nanodots to Nanorods: Oriented aggregation and magnetic evolution of nanocrystalline goethite**
Geophysical Research Letters, v. 30, no. 10, 1512, doi:10.1029/2003GL017021.
High-resolution transmission electron microscopy and low-temperature magnetometry of synthetic goethite nanocrystals show that when aqueous suspensions are aged at 90°C, the nanocrystals grow almost exclusively by oriented aggregation of 3-4 nm primary nanocrystals. These primary particles are superparamagnetic above about 35 K, as shown by variations of magnetic susceptibility with temperature. At low temperature (< 300 K), both remanent and induced magnetizations of primary nanoparticles are about an order of magnitude larger than for micron-sized goethite and can act as magnetic signatures of nanophase in controlled environments.

Isambert, A., Valet, J. P., Gloter, A., and Guyot, F., 2003, **Stable Mn-magnetite derived from Mn-siderite by heating in air**
Journal of Geophysical Research Solid Earth, v. 108, no. B6, 2283, doi:10.1029/2002JB002099.
Magnetic, microscopic and XRD analyses were conducted on oxidation products of Mn-bearing natural crystalline siderite after successive heating steps in air. Newly-formed SD and PSD ferrimagnetic phases have Curie temperatures between 420°C and 560°C. Hematite was detected by XRD after heating the siderite at 480°C, and Mn-ferrite formed at 500°C and persisted even after heating to 700°C. This stable product has a spinel structure with unit cell parameters intermediate between those of magnetite and maghemite, and occurs as single crystals with euhedral shapes of average grain size 90-100 nm.

Errata

The following references were inadvertently omitted from "*Out damned spot!*" (v. 13, n. 1).

Alania MV, A. Gil, and R. Wieliczuk, Statistical analyses of influence of solar and geomagnetic activities on car accident events, *Adv Space Res*, *28*, 673-8, 2001.

Cornelisson, G., F. Halberg, T. Breus, E. Syutkina, R. Baevsky, A. Weydahl, Y. Watanabe, K. Otsuka, J. Siegelova, B. Fiser and E. Bakken, Non-photic solar associations of heart rate variability and myocardial infarction, *Journal of Atmospheric and Solar-Terrestrial Physics*, *64*, 707-720, 2002

Durand-Manterola, H., B, Mendoza, and R. Diaz-Sandoval, Electric currents induced inside biological cells by geomagnetic and atmospheric phenomena, *Adv. Space Res.*, *28*, 679-684, 2001

Keshavan, M., B. Gangadhar, R. Gautam, V. Ajit, and R. Kapur, Convulsive threshold in humans and rats and magnetic field changes: observations during total solar eclipse, *Neuroscience Letters*, *22*, 205-208, 1981

Kirschvink, J. L., A. Kobayashi-Kirschvink, and B. Woodford, Magnetite biomineralization in the human brain, *Proc. Natl. Acad. Sci. USA*, *89*, 7683-7687, 1992

Kirschvink, J. L, M. Walker, and C. Diebel, Magnetite-based magnetoreception [Review], *Current Opinion in Neurobiology, 11(4)*, 462-467, 2001.

Sastre, A., C. Graham, M. Cook, M. Gerkovich, and P. Gailey, Human EEG responses to controlled alterations of the Earth's magnetic field, *Clinical Neurophysiology, 113*, 1382-1390, 2002.

The *Institute for Rock Magnetism* is dedicated to providing state-of-the-art facilities and technical expertise free of charge to any interested researcher who applies and is accepted as a Visiting Fellow. Short proposals are accepted semi-annually in spring and fall for work to be done in a 10-day period during the following half year. Shorter, less formal visits are arranged on an individual basis through the Facilities Manager.

The *IRM* staff consists of **Subir Banerjee**, Professor/Director; **Bruce Moskowitz**, Professor/Associate Director; **Jim Marvin**, Senior Scientist; **Mike Jackson**, Senior Scientist and Facility Manager, and **Peat Sølheid**, Scientist.

Funding for the *IRM* is provided by the **National Science Foundation**, the **W. M. Keck Foundation**, and the **University of Minnesota**.

The *IRM Quarterly* is published four times a year by the staff of the *IRM*. If you or someone you know would like to be on our mailing list, if you have something you would like to contribute (*e.g.*, titles plus abstracts of papers in press), or if you have any suggestions to improve the newsletter, please notify the editor:

Mike Jackson
Institute for Rock Magnetism
University of Minnesota
291 Shepherd Laboratories
100 Union Street S. E.
Minneapolis, MN 55455-0128
phone: (612) 624-5274
fax: (612) 625-7502
e-mail: irm@umn.edu
www.geo.umn.edu/orgs/irm/irm.html

IRM

UNIVERSITY OF MINNESOTA

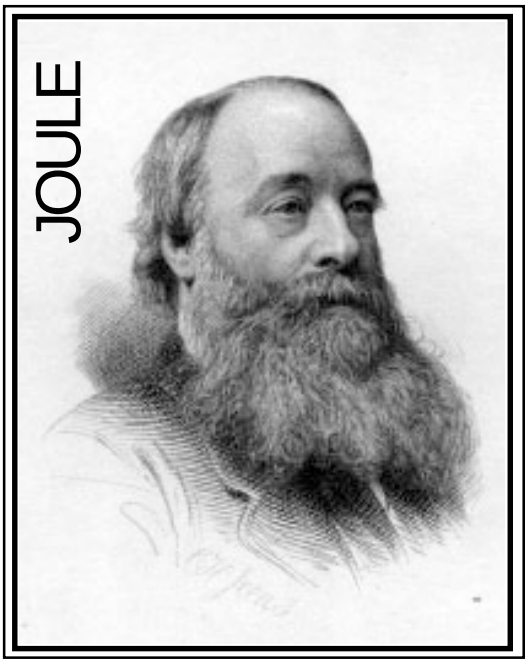

The Scientific Papers of James Prescott Joule
The Physical Society of London, 1884.

Collector's Series #30

Mark Your Calendar:

The dates have been set for the Sixth Santa Fe Conference on Rock Magnetism. Contingent upon funding, the conference will be held June 3-6, 2004, at St. John's College in Santa Fe. Stay tuned for more details. Also planned for next summer is the biennial Czech Castle meeting, June 28 to July 03, 2004. For more information contact Eduard Petrovsky <edp@ig.cas.cz>.

The IRM Quarterly

University of Minnesota
291 Shepherd Laboratories
100 Union Street S. E.
Minneapolis, MN 55455-0128
phone: (612) 624-5274
fax: (612) 625-7502
e-mail: irm@umn.edu
www.geo.umn.edu/orgs/irm/irm.html